

<https://doi.org/10.1038/s42003-025-08197-3>

# Secretory leukocyte protease inhibitor regulates bone metabolism and inflammation in experimental mouse periodontitis



Karin Sasagawa<sup>1,2</sup>, Hisanori Domon<sup>1,3</sup>, Satoru Hirayama<sup>1</sup>, Tomoki Maekawa<sup>1,2,3</sup>, Toshihito Isono<sup>1</sup>, Koichi Tabeta<sup>2</sup> & Yutaka Terao<sup>1,3</sup> 

Periodontitis is characterized by the activity of neutrophil elastase, a host defense factor that leads to the destruction of the epithelial barrier and bacterial invasion of the periodontal tissue. Secretory leukocyte protease inhibitors (SLPI), predominantly secreted by epithelial cells, diffuse into the mucosal surface and inhibit excessive tissue loss caused by elastase during inflammation. The SLPI level is high in healthy gingiva and low in severe periodontitis. In this study, we hypothesized that intragingival administration of SLPI inhibits periodontal tissue destruction caused by periodontitis. Administration of SLPI significantly reduced neutrophil elastase activity in periodontal tissue and alleviated alveolar bone loss in mice. Real-time PCR analysis revealed that SLPI administration downregulated the transcription of pro-inflammatory cytokines and osteoclast-related factors in the gingival tissue. Furthermore, in vitro treatment of bone marrow macrophages with SLPI resulted in the downregulation of osteoclast differentiation. SLPI treatment of MC3T3-E1 cells promoted osteoblast differentiation and bone formation. These findings suggest that SLPI protects against periodontal tissue damage by suppressing inflammation and bone resorption and promoting bone regeneration.

Periodontitis is a chronic inflammatory disease that disrupts periodontal tissue often resulting in tooth loss<sup>1–4</sup>. It is initiated by the formation of dental plaque, which is the adhesion of oral bacteria to the superficial layers of teeth, and the subsequent appearance of pathogenic species. These pathogens enhance inflammatory responses via excessive migration of neutrophils and promotion of inflammatory cytokines production in the periodontal tissue<sup>5</sup>. Additionally, host immune cells and inflammatory cytokines overexpressed in periodontal tissues promote osteoclast activity, leading to alveolar bone resorption<sup>6</sup>. Therefore, in addition to eliminating pathogens, controlling excessive inflammatory responses during periodontal treatment is important.

Neutrophils are the most abundant leukocytes in periodontal pocket and tissues<sup>6,7</sup>. Neutrophils act as host defense factors by phagocytosing and degrading pathogens using the intrinsic protease neutrophil elastase (NE). However, NE leakage from activated neutrophils destroys host tissues through proteolytic activity during inflammatory reactions<sup>8</sup>. Several studies, including our own, have reported that the leaked NE in the periodontal

tissues exacerbates periodontitis as it disrupts the epithelial barrier by cleaving cell adhesion molecules, thereby inducing pathogen invasion and inflammatory progression<sup>9–11</sup>. Notably, a clinical study showed that NE activity in gingival crevicular fluid correlates with periodontitis and may be an indicator of the severity of inflammation<sup>12</sup>. We hypothesized that suppressing NE activity in periodontal tissue might prevent the exacerbation of periodontitis.

Secretory leukocyte protease inhibitor (SLPI) is an 11 kDa multifunctional protein involved in the host defense response expressed by several epithelia, including salivary glands, skin epidermis, and respiratory and digestive organs, primarily in mucosal secretions<sup>13–16</sup>. A critical feature of SLPI is its potent inhibition of serine proteases, including NE, and its suppression of tissue injury<sup>17,18</sup>. SLPI expression is upregulated in response to inflammatory cytokines and bacterial products, and high local levels of SLPI are found in chronic inflammatory diseases, including asthma and arthritis<sup>19,20</sup>. However, clinical findings indicate that SLPI levels are decreased in the saliva and gingival crevicular fluid of patients with severe

<sup>1</sup>Division of Microbiology and Infectious Diseases, Niigata University Graduate School of Medical and Dental Sciences, Niigata, Japan. <sup>2</sup>Division of Periodontology, Niigata University Graduate School of Medical and Dental Sciences, Niigata, Japan. <sup>3</sup>Center for Advanced Oral Science, Niigata University Graduate School of Medical and Dental Sciences, Niigata, Japan. ✉ e-mail: [terao@dent.niigata-u.ac.jp](mailto:terao@dent.niigata-u.ac.jp)

chronic periodontitis<sup>21,22</sup>. Thus, the homeostatic balance between protease and anti-protease factors is disrupted in severe periodontitis.

Our previous study suggested that administration of NE inhibitors suppressed inflammation and alveolar bone loss in mice with periodontitis<sup>23</sup>. In this study, we hypothesized that decreased SLPI expression exacerbates periodontitis, owing to high levels of NE activity in periodontal tissue. We examined the effects of SLPI administration on alveolar bone loss and the gene transcription of inflammatory cytokines and osteoclast differentiation-related factors in the gingiva of a mouse model of periodontitis. We also investigated the effects of SLPI on osteoclast differentiation and osteoblast mineralization in vitro.

## Results

### SLPI expression is downregulated in periodontitis tissue

We analyzed SLPI localization in periodontal tissues using a mouse model of ligature-induced periodontitis. Immunofluorescence analysis revealed that SLPI was expressed in the periodontal ligament in the unligated group, as confirmed by fluorescence immunostaining. Additionally, the fluorescence intensity of SLPI was considerably lower in the ligated group than that in the unligated group (Fig. 1a, b). Real-time PCR analysis showed that the transcription levels of SLPI in periodontal tissues were significantly

lower in the ligated group than in the unligated group (Fig. 1c). These findings are consistent with those of previous studies in humans that reported decreased SLPI expression under periodontal inflammatory conditions<sup>21,22</sup>.

### SLPI suppresses periodontal inflammation and bone resorption induced by tooth ligation

Our previous study suggested that administration of NE inhibitors suppressed inflammation and alveolar bone loss in mice with periodontitis<sup>23</sup>. We examined the effects of SLPI in a mouse model of ligature-induced periodontitis. The maxillary second molars were ligated but the contralateral teeth were not (baseline control). As shown in Fig. 2a, the groups of mice were treated gingivally with phosphate-buffered saline (PBS), SLPI, or the NE inhibitor daily until the day of sacrifice (day 7). In addition, MR16-1, a rat anti-mouse monoclonal IL-6 receptor antibody<sup>24</sup>, and Bone morphogenetic protein 2 (BMP-2), which can induce osteogenic differentiation<sup>25,26</sup>, were administered to the mouse model as controls. MR16-1 treatment suppressed the infiltration of immune cells after spinal cord injury, and increased post-injury locomotor function<sup>27</sup>. On the other hand, BMP-2 has been shown to promote bone formation in the maxilla of mice<sup>25</sup>. Fig. 2b, c, significant bone resorption was induced in the ligated + PBS group, whereas

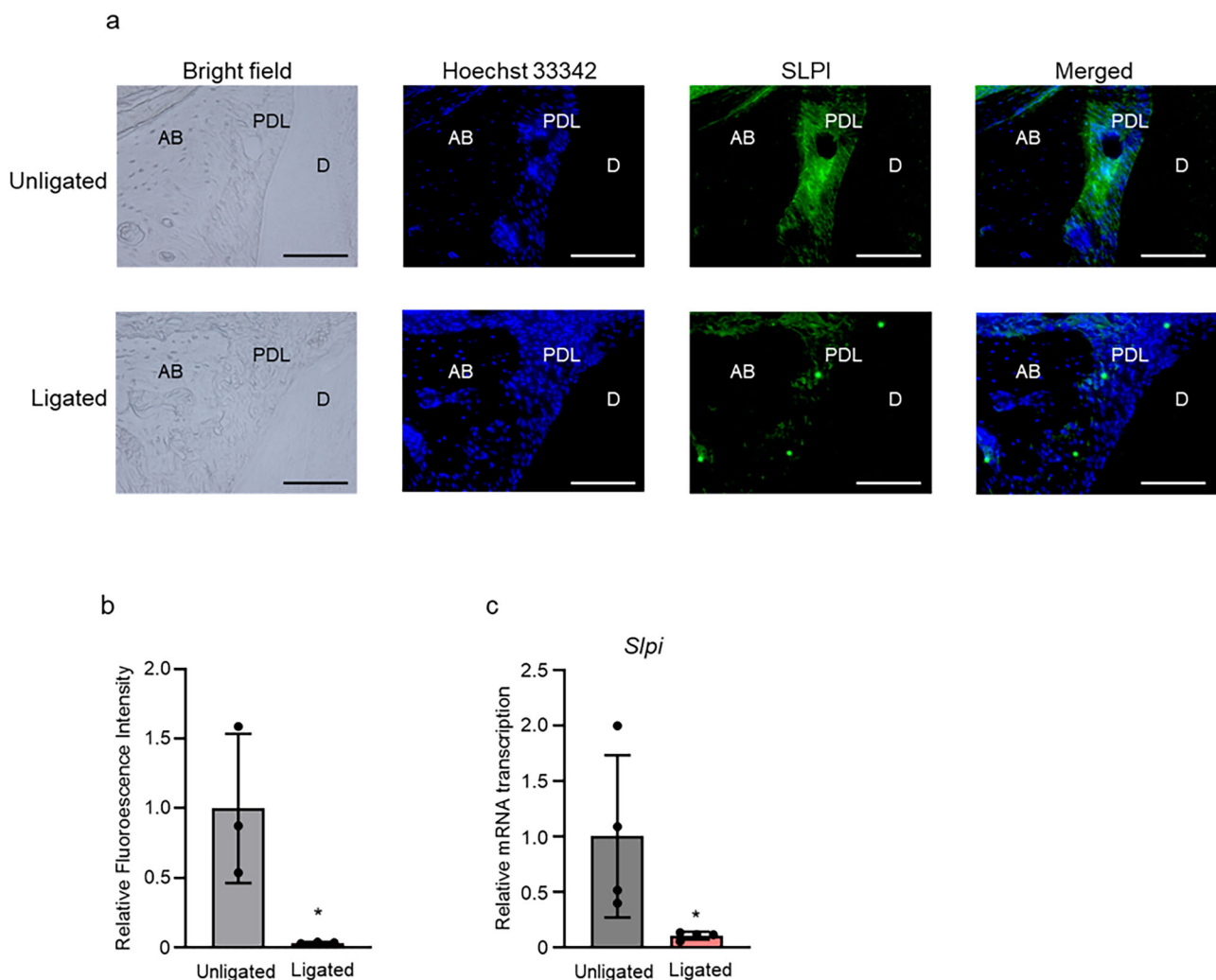


**Fig. 1 | SLPI expression is decreased in murine periodontitis tissue. a** Frozen maxillae sections from a ligature-induced murine model of periodontitis were stained with anti-SLPI antibody (green) and Hoechst 33,342 (nucleus; blue). Representative fluorescence images are shown. Scale bar: 50  $\mu$ m. **b** The fluorescence intensity of SLPI in the unligated or ligated murine palatal gingiva was calculated

( $n = 3$ ). Data represent the mean  $\pm$  SD and were evaluated using Student's  $t$  test; \* $P < 0.05$ . **c** Transcription levels of *Slpi* in murine palatal gingiva were determined by real-time PCR. Relative mRNA levels were normalized to those of *Gapdh* ( $n = 4$ ). All data are presented as mean  $\pm$  SD. Statistical analysis was performed using Student's  $t$  test; \* $P < 0.05$ . AB, alveolar bone; D, dentine; PDL, periodontal ligament.

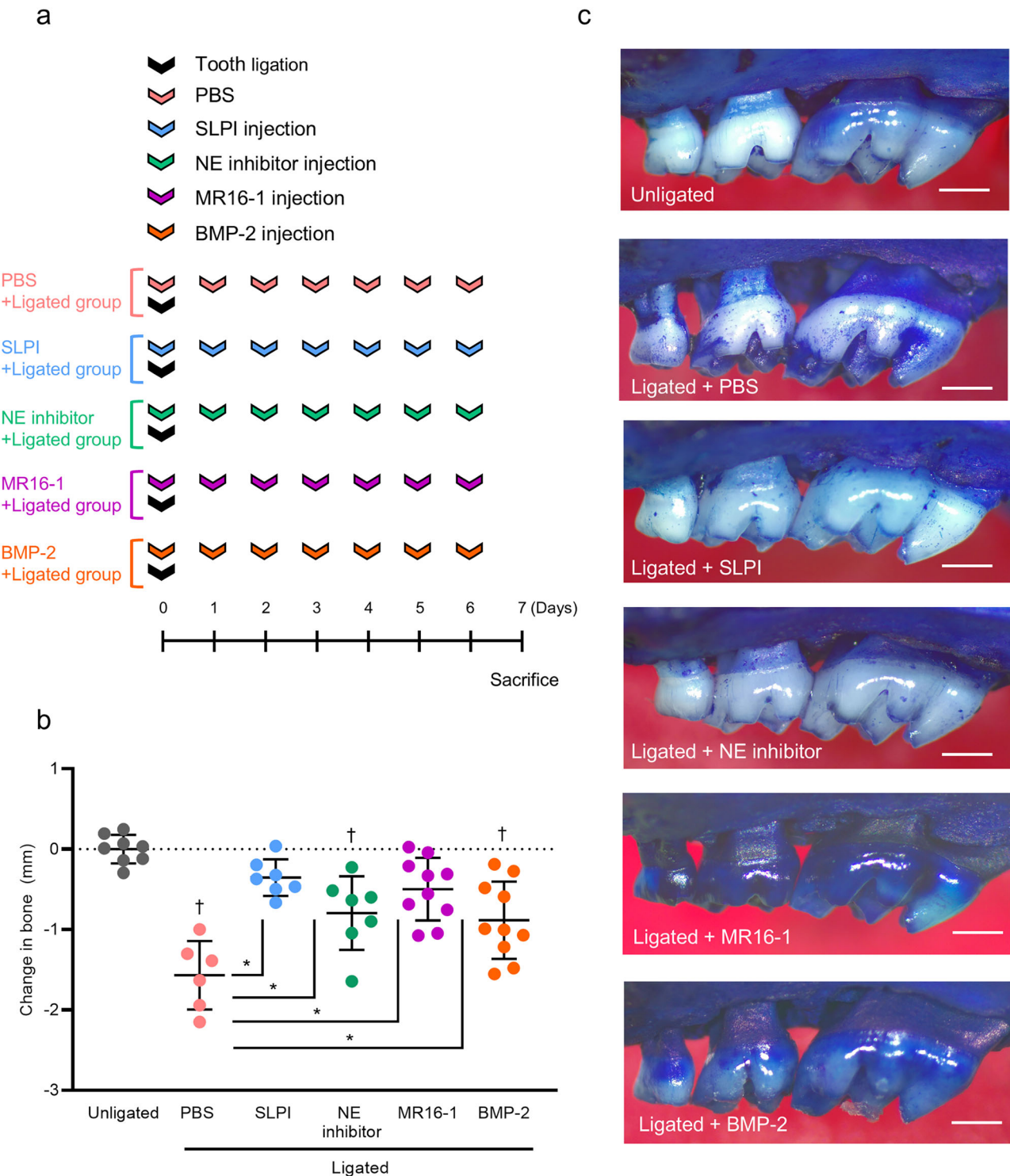


**Fig. 2 | SLPI inhibits alveolar bone loss in murine periodontitis model.**

**a** Experimental design. **b** Periodontal bone loss assessed using stereoscopic microscopy. Negative values indicate bone loss relative to the unligated group ( $n = 6-10$ ). **(c)** Representative stereoscopic microscopy images Scale bar: 0.5 mm. Data

represent the mean  $\pm$  SD and were evaluated using a one-way analysis of variance with Tukey's multiple comparison test.  $*P < 0.05$ .  $^{\dagger}$ Significantly different at  $P < 0.05$  when compared to the unligated group.

the administration of SLPI, the NE inhibitor, MR16-1, or BMP-2 significantly attenuated bone loss. Notably, the bone resorption levels were found to be not significantly different between the ligated + SLPI and unligated groups. Although NE activity in gingival tissues significantly increased after tooth ligation, SLPI or NE inhibitor administration significantly reduced NE activity (Fig. 3a). Transcription of proinflammatory cytokines, *Il6* and *Il1b* was increased in the gingiva of the ligated + PBS

group compared to that in the unligated group (Fig. 3b). In addition, administration of SLPI or NE inhibitors significantly downregulated the transcription of these genes in the gingiva. In contrast, the transcription of *Il10*, anti-inflammatory cytokine, was increased in the gingiva of the ligated + SLPI group when compared to that in the other groups. Notably, the transcription of *Slpi* also increased in mouse gingival tissues compared to that in the ligated + PBS group. These findings suggest that the intragingival

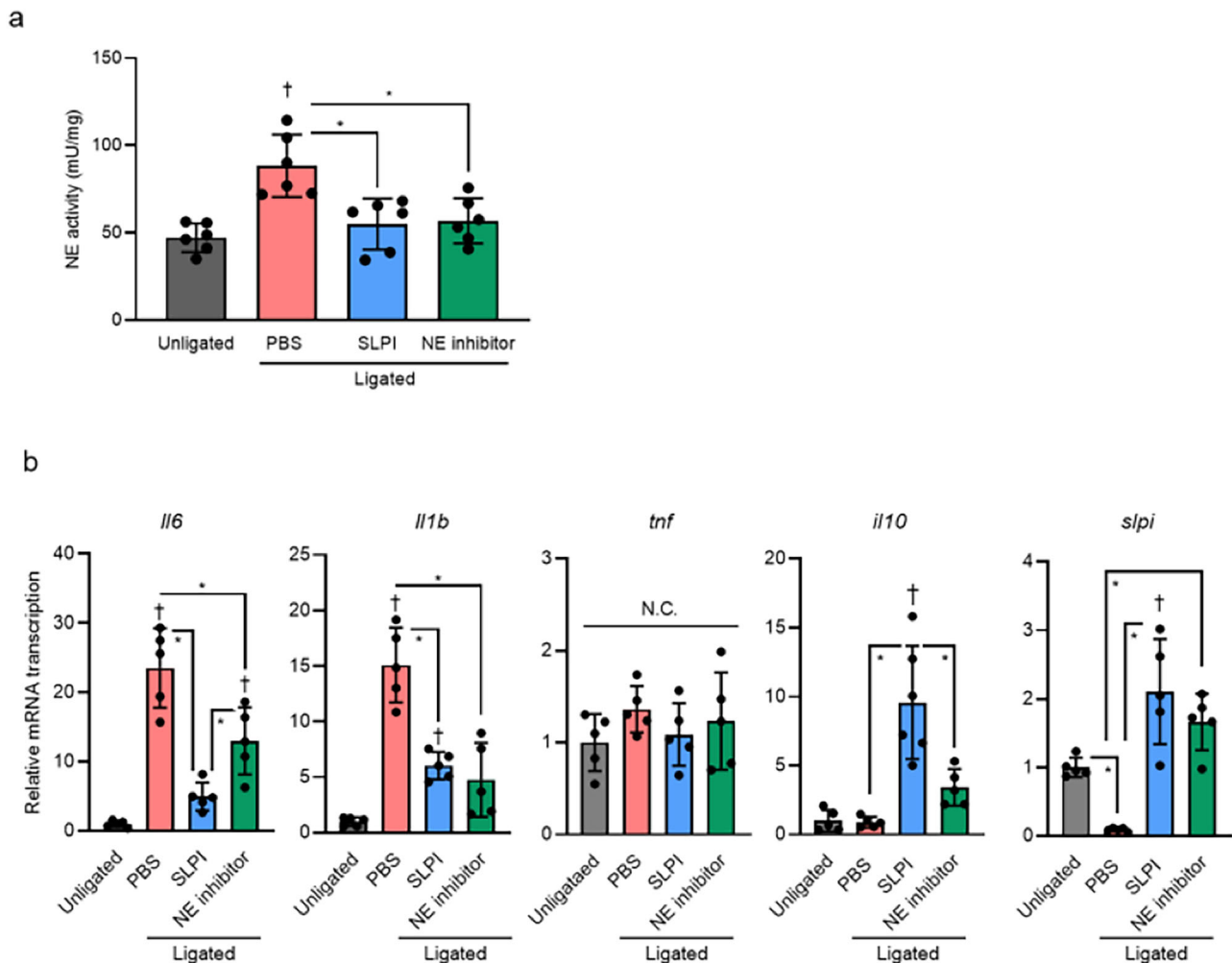


**Fig. 3 | SLPI effect neutrophil elastase activity and gene transcription of proinflammatory cytokines in murine gingiva. a** NE activity in the supernatants from the homogenized palatal gingiva was evaluated ( $n = 6$ ). **b** Transcription levels of *Il6*, *Il1b*, *Tnf*, *Il10*, and *Slpi* genes in the murine palatal gingiva were determined by real-time PCR. Relative mRNA levels were normalized to those of *Gapdh* ( $n = 5$ ). All data

are presented as mean  $\pm$  SD. Statistical analysis was performed using one-way analysis of variance with Tukey's multiple comparison test.  $*P < 0.05$ .  $^{\dagger}$ Significantly different at  $P < 0.05$  compared to the unligated group.  $*P < 0.05$ .  $^{\dagger}$ Significantly different at  $P < 0.05$  compared to the unligated group.

administration of SLPI minimizes alveolar bone loss, downregulates the transcription of proinflammatory cytokine genes, and upregulates anti-inflammatory cytokine genes.

### SLPI decreased the number of osteoclasts in the periodontal ligament tissue

Next, we investigated the effects of SLPI on osteoclast differentiation in periodontal tissues. Figure 4a, b show a significant increase in the number of tartrate-resistant acid phosphatase (TRAP)-positive cells around the second molars in the ligated + PBS group compared with the unligated group. Consistent with the amount of alveolar bone resorption, the administration of SLPI or NE inhibitor significantly reduced the number of TRAP-positive cells in periodontal tissue compared with that in the ligated + PBS group. Additionally, SLPI administration significantly downregulated the transcription of nuclear factor of activated T cells C1 (*Nfatc1*) and *Rank*, which are osteoclast differentiation factors, compared to the ligated + PBS group, whereas the transcription of *Acp5* and *Ctsk*, which are bone resorption activity-related factors, was significantly downregulated by SLPI or NE inhibitor administration (Fig. 4c). The ligated + SLPI group showed significant downregulation of the transcription of *Rank* compared to the ligated + NE inhibitor group. Therefore, the inhibition of bone resorption by SLPI (Fig. 2b) may be associated with a decrease in the number of osteoclasts in the periodontal ligament tissue.

### SLPI suppresses osteoclast differentiation and bone resorption activity in vitro

Figure 2b shows that alveolar bone resorption levels in the ligated + SLPI group were comparable to those in the ligated + MR16-1 and ligated + BMP-2 groups. In addition, there was a significant difference in the number of osteoclasts around the periodontal ligament between the ligated+PBS and ligated+SLPI groups. Bone marrow-derived macrophages (BMMs) differentiated into multinuclear osteoclasts in the presence of macrophage colony-stimulating factor (M-CSF) and nuclear factor- $\kappa$ B ligand activating factor (RANKL). Figure 5a, b demonstrate that the treatment of BMMs with SLPI resulted in a reduction in the number of TRAP-positive cells. Subsequently, using fluoresceinamine-labeled sodium chondroitin poly-sulfate/calcium phosphate (FACPS/CaP)-coated plates, we examined the effect of SLPI on the bone resorption activity of BMMs. When cultured on labeled CaPs stimulated with M-CSF and RANKL, BMMs differentiate into osteoclasts, and the fluorescent intensity of the culture supernatant is consistent with the bone resorption activity of BMMs<sup>28</sup>. The fluorescence intensity was significantly decreased in the culture supernatant from the SLPI-treated group compared to that in the medium-only group (Fig. 5c). Additionally, in the SLPI-treated group, the transcription of *Nfatc1* and *Rank* was significantly downregulated when compared to that in the medium-only group, whereas no significant differences were observed for *Acp5* and *Ctsk* (Fig. 5d). It has been reported that *Acp5* and *Ctsk* are



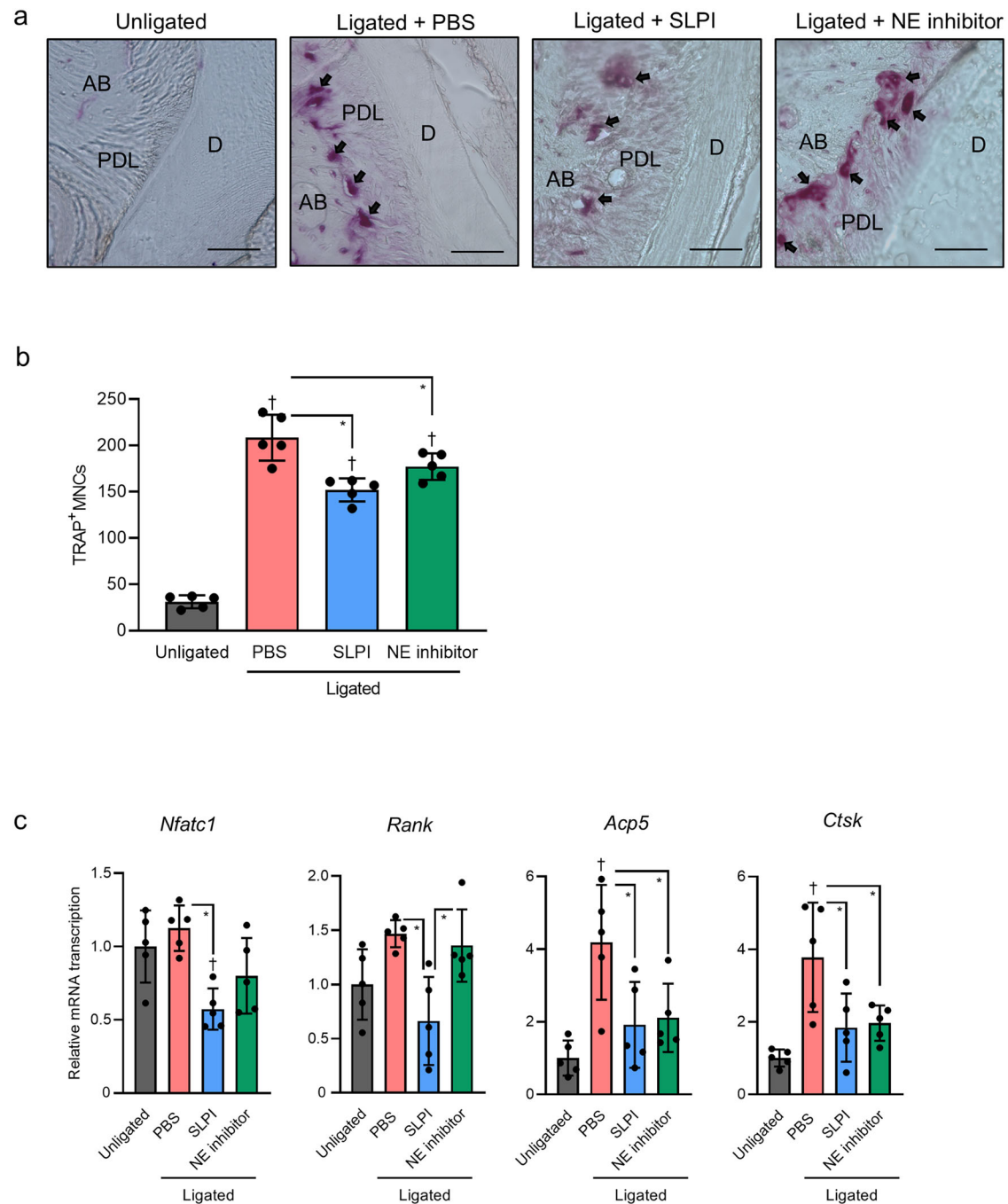


**Fig. 4 | SLPI inhibits osteoclast differentiation in murine periodontitis model.** **a** Frozen maxillae sections were stained with tartrate-resistant acid phosphatase (TRAP). Representative images obtained by optical microscopy are shown; arrows indicate TRAP-positive osteoclasts. AB, alveolar bone; D, dentine; PDL, periodontal ligament. Scale bars, 50  $\mu$ m. **b** TRAP-positive multinucleated cells (MNCs) were counted in six coronal sections of ligated sites of each mouse ( $n = 5$ ). **c** Transcription

levels of osteoclast-related factors in the murine palatal gingiva were determined by real-time PCR. Relative mRNA levels were normalized to those of *Gapdh* ( $n = 5$ ). All data are presented as mean  $\pm$  SD. Statistical analysis was performed using one-way ANOVA followed by Tukey's multiple comparisons test. \* $P < 0.05$ . †Significantly different at  $P < 0.05$  compared to the unligated group.

expressed in the terminal differentiation of osteoclasts and affect their bone resorption ability<sup>25</sup>. These data suggest that SLPI inhibits the initial formation of osteoclasts.

### SLPI promotes osteoblast differentiation and mineralization in vitro

We investigated the effect of SLPI on osteoblast differentiation and bone formation. MC3T3-E1 cells are most commonly used as an in vitro model of bone mineralization, and the collagenous extracellular matrix synthesized

by the cell line and its organization and mineralization is very similar to what occurs in the bone<sup>29,30</sup>. After MC3T3-E1 cells were cultured in osteoblast differentiation medium for 5 days, staining for alkaline phosphatase (ALP), a marker of osteoblast maturation, was performed to evaluate osteoblast differentiation. ALP activity was enhanced in the SLPI-treated group compared to that in the untreated and NE inhibitor-treated groups (Fig. 5e, f). Additionally, when mineralized nodule formation were detected in MC3T3-E1 cells cultured for 22 days by Alizarin Red staining, the amount of mineral nodule formation significantly increased in the SLPI-treated

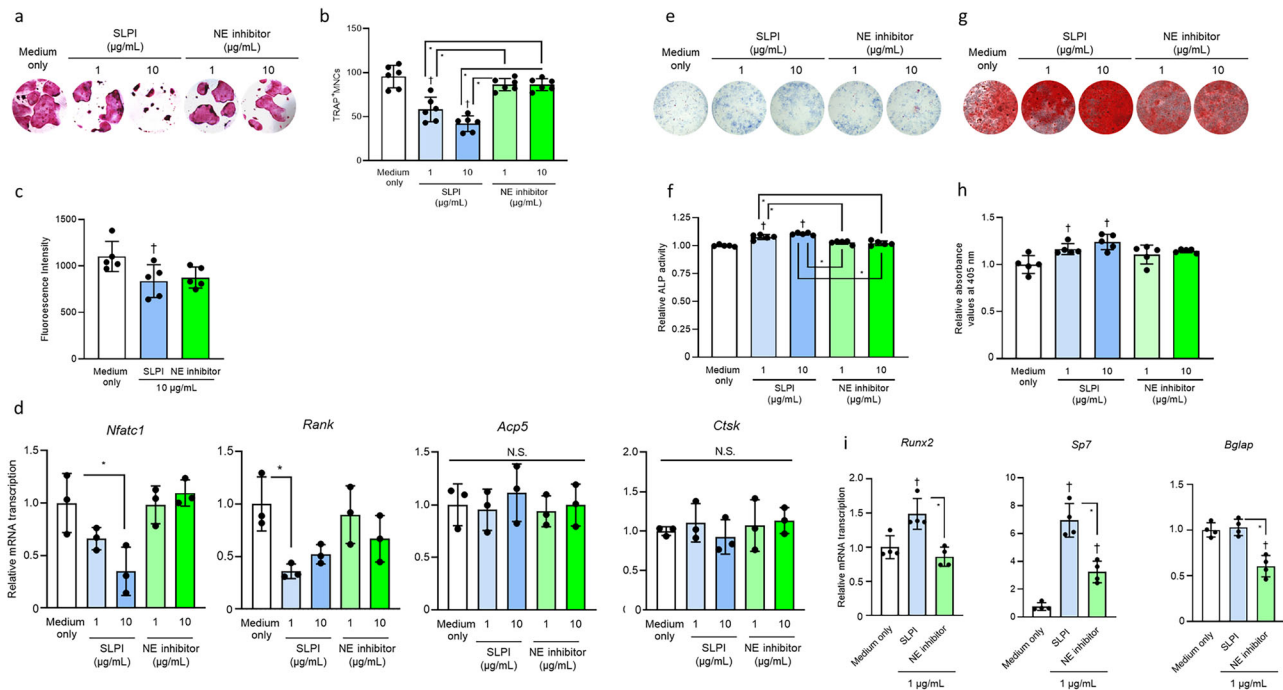


**Fig. 5 | SLPI suppresses osteoclast differentiation and enhances osteogenic mineralization in vitro.** **a–d** Bone marrow-derived macrophages (BMMs) were cultured in the presence of M-CSF (100 ng/mL) and RANKL (100 ng/mL). **a** Representative images of TRAP-positive MNCs obtained by optical microscopy are shown. **b** TRAP-positive MNCs per well were counted ( $n = 6$ ). **c** BMMs were cultured on the fluoresceinamine-labeled sodium chondroitin poly-sulfate/calcium phosphate-coated plates in the presence of M-CSF (100 ng/mL) and RANKL (100 ng/mL). The absorption activity was examined by measuring the fluorescence intensity of the culture supernatant after 7 days ( $n = 5$ ). **d** Transcription of the genes encoding osteoclast-related factors was analyzed by real-time PCR. Data were normalized to *Gapdh* mRNA. (**e–i**) The osteogenic mineralization was determined

in MC3T3-E1 osteoblastic progenitors in the presence of mice SLPI (1–10  $\mu\text{g/mL}$ ), or NE inhibitor (1–10  $\mu\text{g/mL}$ ). **e** Representative images of MC3T3-E1 cells by alkaline phosphatase (ALP) staining after 5 days. **f** Quantification of ALP activity using ImageJ software ( $n = 5$ ). **g** Representative images of mineralized nodule formation in MC3T3-E1 cells, detected by Alizarin Red S staining. **h** Alizarin Red S-stained calcified deposits were extracted and quantified by spectrophotometry at 405 nm ( $n = 5$ ). **i** Analysis of *Runx2* (day 3), *Sp7* (day 9), *Bglap* (day 12) by real-time PCR, normalized to *Gapdh* ( $n = 4$ ). All data are presented as mean  $\pm$  SD. Statistical analysis was performed using one-way ANOVA followed by Tukey's multiple comparisons test. \* $P < 0.05$ . †Significantly different compared to the medium-only group ( $P < 0.05$ ).

group (Fig. 5g, h). In the SLPI-treated group, there was a significant increase in the expression of master osteogenic transcription factor *Runx2* and *Sp7*, which are typical early and middle osteogenic markers<sup>31</sup>, compared to the medium-only group; however, no significant difference was observed in the transcription of bone  $\gamma$ -carboxyglutamic acid-containing protein (*Bglap*), a late-stage osteoblast marker (Fig. 5i). These results show that SLPI promotes osteoblast differentiation in MC3T3-E1 cells from the early to mid-stage, and that this results in the induction of mineralization.

## Discussion

In this study, we found that SLPI significantly inhibited NE activity and alveolar bone loss in experimental periodontal tissues. These findings support the concept that SLPIs exert periodontitis-preventive effects via protease inhibition. Although SLPI is a multifunctional protein that has recently been reported to be involved in bone metabolism<sup>32</sup>, its function remains unclear. We found that SLPI suppressed osteoclast differentiation of BMMs and promoted osteoblast differentiation and mineralization of MC3T3-E1 cells. Therefore, we suggest that the inhibitory effect of SLPI on periodontal tissue destruction is due to its protease inhibitory effect and ability to regulate bone-resorbing osteoclasts and bone-forming osteoblasts.

Excessive extracellular NE released from neutrophils exacerbates by destroying epithelial tissues and alveolar bone via the spread of bacterial infections<sup>11</sup>. Additionally, clinical evidence suggests that NE induces inflammation progression and contributes to the severity of periodontitis<sup>10</sup>. Previous studies have demonstrated that selective NE inhibition using Sivelestat, in a ligature-induced periodontitis mouse model suppressed the transcription of inflammatory cytokine genes such as IL-6 in periodontal

tissues and reduced alveolar bone loss<sup>9,23</sup>. Therefore, NE inhibition holds promise as a potential treatment for inflammatory diseases such as periodontitis. In the present study, we have investigated the effects of the administration of an anti-mouse IL-6 receptor antibody (MR16-1)<sup>33</sup> and a bone morphogenetic protein, BMP-2<sup>25</sup>, on inflammation-induced alveolar bone resorption in a mouse periodontitis model. The administration of MR16-1 or BMP-2 reduced alveolar bone loss. Consistent with these findings, our study demonstrated that SLPI suppressed NE activity, transcription of inflammatory cytokine genes, and alveolar bone loss in periodontal tissues.

Alveolar bone loss in periodontitis is mediated by host immune and inflammatory responses to the pathogen<sup>34,35</sup>. Normal bone remodeling depends on an exquisite balance between bone resorption and bone formation, but inflammation-induced cytokines such as IL-6 and IL-1 cause a shift of bone homeostasis toward bone resorption in periodontitis<sup>5,36,37</sup>. Therefore, the treatment of periodontitis requires the arrest of the inflammatory process by eliminating the infection and controlling bone metabolism by osteoclasts and osteoblasts. Although the functional role of SLPI in bone resorption has not been reported, in this study, we showed that treatment of BMMs with SLPI inhibited osteoclast differentiation in vitro. SLPI is a regulator of nuclear factor kappa B (NF- $\kappa$ B) in monocytic cells<sup>17,38</sup>, and the transcription of nuclear factor of activated T cells c1 (*Nfatc1*), an important target of NF- $\kappa$ B<sup>39</sup>, was decreased in BMMs treated with SLPI, suggesting that SLPI inhibits osteoclast differentiation via NF- $\kappa$ B signaling. On the other hand, it has been suggested that SLPI expressed in osteoblasts may promote bone formation by regulating gene transcription of osteogenic genes, including the master transcription factors runt-related transcription

factor-2 (*Runx2*), osteolytic factor (*Sp7*), bone  $\gamma$ -carboxyglutamic acid-containing protein (*Bglap*)<sup>32,40</sup>. In the present study, the treatment of MC3T3-E1 cells with SLPI promoted osteoblast differentiation and mineralization. We investigated bone resorption by osteoclasts and osteoblastic differentiation and demonstrated that SLPI exerts distinct effects on each process.

This study has some limitations. Here, periodontitis was induced in parallel with SLPI administration. However, in clinical practice, periodontal treatment is often initiated after alveolar bone resorption due to inflammation<sup>3</sup>, making it difficult to directly apply the results of our study to clinical practice. To mimic the pathophysiology of active periodontitis, acute inflammation in periodontal tissues was induced by ligating the teeth of mice. By simultaneously initiating SLPI administration at the same time, our experimental results suggest the potential of SLPI treatment to inhibit periodontal tissue destruction caused by active periodontitis. Additionally, as SLPI affected both bone resorption and formation, further analysis is needed to investigate the effects of SLPI on alveolar bone defects.

In conclusion, this study demonstrated that SLPI exhibits anti-protease activity in vivo, suppresses bone resorption in vivo and in vitro, and enhances bone formation in vitro. Further investigations into the regulatory mechanisms of SLPI and its use in bone metabolism could potentially expedite the development of novel therapeutic approaches for periodontitis.

## Materials and methods

### Mice and reagents

Male 7- to 8-week-old BALB/cA mice were purchased from CLEA Japan, Inc. (Tokyo, Japan), maintained under standard conditions in individual cages, and provided with sterile food and water ad libitum. All animal experiments were approved by the Institutional Animal Care and Use Committee of the Niigata University (approval no. SA00181). Sivelestat, a NE inhibitor, was purchased from Ono Pharmaceutical Co., Ltd. (Osaka, Japan). It was dissolved in phosphate buffered saline (PBS) to a final concentration of 10 mg/mL. Bone morphogenetic protein 2 (BMP-2) was purchased from Biologend, USA. The anti-mouse IL-6 receptor antibody (MR16-1) was supplied from Chugai Pharmaceutical Co., Ltd. (Tokyo, Japan) and Professor Tadimitsu Kishimoto (Osaka University). BMP-2 and MR16-1 were dissolved in PBS.

### Construction of recombinant mouse SLPI

Recombinant mouse SLPI was constructed as previously described with some modifications<sup>41</sup>. Mouse SLPI DNA (accession number: NP\_035544) was synthesized by Eurofins Genomics. The ORF of SLPI was amplified from the synthetic DNA using forward primer 5'-GTCGCATGCCCCCTGGACTGTGGAAGGAG-3' and reverse primer 5'-GTTC TGCAGTCACATCGGGGCGAG-3'. SphI-PstI site of the pQE-30 vector (QIAGEN). *Escherichia coli* Rosetta-gami B (DE3) strain (Novagen) was transformed with the plasmid and transformants were incubated at 30 °C for 16 h in the presence of 1 mM isopropyl- $\beta$ -D-thiogalactopyranoside (FUJIFILM Wako Pure Chemical). Recombinant SLPI expressed in the insoluble fraction was solubilized in a lysis buffer containing 6 M guanidine hydrochloride, 500 mM NaCl, 10 mM imidazole, and 20 mM sodium phosphate (pH 7.8), and recombinant SLPI was purified using Ni-NTA agarose (QIAGEN). Active recombinant SLPI was obtained by dialyzing recombinant SLPI purified under denaturing conditions in a refolding buffer containing 0.5 M urea, 0.4 M L-arginine, 0.5 mM GSSG, 150 mM NaCl, and 50 mM Tris-HCl at 4 °C for 16 h and finally replacing the buffer with PBS.

### Mouse Tooth Ligated Model

To establish this model, a 5-0 silk ligature (Akiyama MEDICAL MFG. Co. Ltd., Tokyo, Japan) was tied around the maxillary second molar to induce periodontitis<sup>42</sup>. Thereafter, 50  $\mu$ g NE inhibitor in 5  $\mu$ L PBS (ligature + NE inhibitor group), 500 ng recombinant mouse SLPI in 5  $\mu$ L PBS (ligature + SLPI group), 500 ng recombinant MR16-1 in 5  $\mu$ L PBS (ligature + MR16-1

group), BMP-2 in 5  $\mu$ L PBS (ligature + BMP-2 group) or 5  $\mu$ L PBS was injected into the palatal gingiva of the molar once daily for 7 days for other analyses. All animal experiments were conducted by a researcher who analyzed the results and was blinded to the experiment. The humane endpoint was decided as 20% reduction in body weight from baseline or signs of intense pain.

### NE activity assay

NE activity in the palatal gingival tissues of mice has been described previously<sup>23</sup>. Three hours after the last injection of mouse SLPI, NE inhibitor, or PBS, palatal gingival tissues were homogenized in Tris-HCl buffer (pH 0.8) using a BioMasher (Nippi, Tokyo, Japan). The samples were centrifuged at 300  $\times$  g for 3 min, and the NE activity in the supernatant was determined using *N*-methoxysuccinyl-Ala-Ala-Pro-Val *p*-nitroanilide (Merck Millipore, Billerica, MA, USA). Samples were incubated in 0.1 M Tris-HCl buffer containing 0.5 M NaCl and 1 mM substrate at 37 °C for 24 h, and then absorbance at 405 nm was measured.

### Measurement of periodontal bone loss

Each maxilla was skinned, then dry skulls were stained with methylene blue (5% in water) for 5 min. Periodontal bone loss in the maxilla was morphometrically assessed using a stereoscopic microscope (Leica Microsystems, Wetzlar, Germany). According to a previously described method<sup>42</sup>, the distance from the cement-enamel junction to the alveolar bone crest was measured at six predetermined sites on the ligated second molar and adjacent affected regions. Bone change was calculated by subtracting the sum of the cement-enamel and the alveolar bone crest values from the six corresponding values in the unligated area. Negative values (mm) indicate bone loss relative to baseline (unligated control).

### Histologic analysis

The maxillae prepared from the murine model were fixed in a 4% paraformaldehyde solution (FUJIFILM Wako Pure Chemical Corporation, Osaka, Japan) for 24 h. The specimens were decalcified in decalcifying solution B (Wako Pure Chemical Industries) for 1 week at 4 °C. The specimens were then embedded in the O.C.T. compound (Sakura Finetek, Torrance, CA, USA) and frozen in liquid nitrogen. The coronal sections were prepared using a cryostat (Leica Biosystems). The prepared coronal sections (10  $\mu$ m) were stained with tartrate-resistant acid phosphatase (TRAP) staining (Cosmo Bio Co., Tokyo, Japan).

### Immunofluorescence

SLPI expression in frozen coronal sections was assessed by immunofluorescence using an SLPI-specific antibody (Novus Bio, Centennial, USA). After overnight incubation with the primary antibody at 4 °C, SLPI was visualized using Alexa Fluor 488 conjugated anti-rabbit secondary antibody (Invitrogen, Carlsbad, CA). Nuclei were identified using Hoechst33342 for 15 min at 37 °C. Sections were observed under a confocal laser scanning microscope (Carl Zeiss, Jena, Germany). Additionally, the fluorescence intensity of SLPI was calculated using BZ-9000 analysis software (Keyence, Osaka, Japan).

### Osteoclast differentiation assay using murine bone marrow macrophages

As described previously<sup>43</sup>, BMMs were collected from the femurs and tibias of mice and age-matched unligated mice were used as controls under sterile conditions. Briefly, BMMs were cultured in 96-well plates (1.0  $\times$  10<sup>5</sup> per well) with recombinant macrophage colony-stimulating factor (M-CSF) (30 ng/mL; R&D Systems, Minneapolis, MN, USA) for 3 h in minimum essential medium alpha (MEM $\alpha$ ; Wako Pure Chemical Co., Tokyo, Japan) with 10% fetal bovine serum (FBS) at 37 °C in 5% CO<sub>2</sub>. After removing nonadherent cells, adherent cells were further cultured in MEM $\alpha$  media supplemented with 10% FBS, 100 ng/mL recombinant soluble receptor activator of nuclear factor-kappa B ligated (RANKL; R&D Systems), and 100 ng/mL M-CSF in the presence or absence of recombinant mice



SLPI (1 or 10 µg/mL) or NE inhibitor (1 or 10 µg/mL) for 7 days. The medium was replaced with a fresh solution every three days during the incubation period. Multinucleation of osteoblasts was confirmed by TRAP staining (to confirm multinucleation). To determine the effect of SLPI on the absorption activity, BMMs were cultured in FACPS/CaP-coated 96-well plates (200 µL/well) (PG Research Co., Ltd., Tokyo, Japan). After 7 days, the supernatant was collected and fluorescence intensity (excitation: 485 nm, emission: 535 nm) was measured using GloMax (Promega Corporation, Madison, WI, USA)<sup>28</sup>.

### Osteoblastogenesis assay

The murine osteoblastic progenitor cell line, MC3T3-E1, was obtained from the RIKEN Bioresource Center (RCB1126). MC3T3-E1 cells were maintained in MEMα media supplemented with 10% FBS and penicillin-streptomycin solution (×100) (Wako Pure Chemical Co.) at 37 °C in 5% CO<sub>2</sub>. To determine the osteogenic differentiation, cells were cultured with 50 µg/mL ascorbic acid (Wako Pure Chemical Co.) and 10 mM β-glycerophosphate (Wako Pure Chemical Co.) in MEMα media supplemented with 10% FBS. The cell culture medium was replaced every three days. ALP activity after five days was detected using an ALP staining kit (Cosmo Bio Co., Ltd. Tokyo, Japan) and photographed under a stereoscopic microscope (Leica Microsystems, Wetzlar, Germany) (25×). The ALP-positive area was quantified using the ImageJ software version 1.53t (National Institute of Health, Bethesda, MD, USA). Mineralization of bone nodules was detected by staining with Alizarin Red S (Wako Pure Chemical Co.) 24 days after the differentiation of MC3T3-E1 cells. Alizarin Red S-stained calcified deposits were extracted using formic acid and quantified by measuring the optical density at 405 nm using a microplate reader.

### Quantitative real-time PCR

Total RNA was extracted from mouse maxillary palatal gingiva, BMMs, or MC3T3-E1 cells using TRI reagent (Molecular Research Center, Inc., Cincinnati, OH, USA). RNA was reverse-transcribed using ReverTra Ace qPCR RT Master Mix (TOYOBO Co., Ltd., Osaka, Japan). Quantitative PCR with cDNA was performed according to the manufacturer's protocol using a Step One Plus real-time PCR system (Thermo Fisher Scientific). The data was analyzed using the comparative CT (ΔΔCT) method. TaqMan probes and primers for the expression of housekeeping gene (*Gapdh*, Mm99999915\_g1) along with *Il6* (Mm00434228\_m1), *Il1b* (Mm00434228\_m1), *Nfatc1* (Mm01265944\_m1), and *Tnfrsf11a* (*Rank*, Mm00437132\_m1), *Acp5* (Mm00475698\_m1), *Ctsk* (Mm00484039\_m1), *Runx2* (Mm00501584\_m1), *Sp7* (Mm00504574\_m1), *Bglap* (Mm03413826\_mH) were purchased from Thermo Fisher Scientific.

### Statistical and reproducibility

All data are presented as mean ± SD, as indicated in the figure legends. Statistical analyses were performed using GraphPad Prism 8.4.3 (GraphPad Software, La Jolla, CA, USA). One-way ANOVA followed by Dunnett's or Tukey's multiple comparison test was used, with \**P* < 0.05 considered statistically significant. Animal experiments were conducted using mice that were randomly assigned to experimental groups to minimize bias. Sample size was based on prior studies using similar models; no formal power calculation was performed. All in vivo and in vitro experiments were independently repeated two to three times, and quantitative data were obtained from at least three (*n* = 3–5) independent experiments to ensure reproducibility.

### Reporting summary

Further information on research design is available in the Nature Portfolio Reporting Summary linked to this article.

### Data availability

The authors confirm that the data supporting the findings of this study are available within the article. All source data underlying graphs can be obtained in Supplementary data.

Received: 25 December 2023; Accepted: 8 May 2025;

Published online: 16 May 2025

### References

1. Slots, J. Periodontitis: facts, fallacies and the future. *Periodontol.* **2000** **75**, 7–23 (2017).
2. Kwon, T., Lamster, I. B. & Levin, L. Current concepts in the management of periodontitis. *Int. Dent. J.* **71**, 462–476 (2021).
3. Kinane, D. F., Stathopoulou, P. G. & Papapanou, P. N. Periodontal diseases. *Nat. Rev. Dis. Prim.* **3**, 17038 (2017).
4. Sanz, M. et al. Treatment of stage I–III periodontitis—The EFP S3 level clinical practice guideline. *J. Clin. Periodontol.* **47**, 4–60 (2020).
5. Hienz, S. A., Paliwal, S. & Ivanovski, S. Mechanisms of bone resorption in periodontitis. *J. Immunol. Res.* **2015**, 615486 (2015).
6. Scott, D. A. & Krauss, J. Neutrophils in periodontal inflammation. *Front. Oral Biol.* **15**, 56–83 (2012).
7. Sculean, A., Chapple, I. L. & Giannobile, W. V. Wound models for periodontal and bone regeneration: the role of biologic research. *Periodontol.* **2000** **68**, 7–20 (2015).
8. Watanabe, H., Hattori, S., Katsuda, S., Nakanishi, I. & Nagai, Y. Human neutrophil elastase: degradation of basement membrane components and immunolocalization in the tissue. *J. Biochem.* **108**, 753–759 (1990).
9. Hiyoshi, T. et al. *Aggregatibacter actinomycetemcomitans* induces detachment and death of human gingival epithelial cells and fibroblasts via elastase release following leukotoxin-dependent neutrophil lysis. *Microbiol. Immunol.* **63**, 100–110 (2019).
10. Lee, W., Aitken, S., Sodek, J. & McCulloch, C. A. Evidence of a direct relationship between neutrophil collagenase activity and periodontal tissue destruction in vivo: role of active enzyme in human periodontitis. *J. Periodontol. Res.* **30**, 23–33 (1995).
11. Hirschfeld, J. Neutrophil subsets in periodontal health and disease: a mini review. *Front. Immunol.* **10**, 3001 (2019).
12. Bader, H. I. & Boyd, R. L. Long-term monitoring of adult periodontitis patients in supportive periodontal therapy: correlation of gingival crevicular fluid proteases with probing attachment loss. *J. Clin. Periodontol.* **26**, 99–105 (1999).
13. Majchrzak-Gorecka, M., Majewski, P., Grygier, B., Murzyn, K. & Cichy, J. Secretory leukocyte protease inhibitor (SLPI), a multifunctional protein in the host defense response. *Cytokine Growth Factor Rev.* **28**, 79–93 (2016).
14. Lee, C. H. et al. Distribution of secretory leukoprotease inhibitor in the human nasal airway. *Am. Rev. Respir. Dis.* **147**, 710–716 (1993).
15. Wiedow, O., Harder, J., Bartels, J., Streit, V. & Christophers, E. Antileukoprotease in human skin: an antibiotic peptide constitutively produced by keratinocytes. *Biochem. Biophys. Res. Commun.* **248**, 904–909 (1998).
16. Abe, T. et al. Expression of the secretory leukoprotease inhibitor gene in epithelial cells. *J. Clin. Invest.* **87**, 2207–2215 (1991).
17. Nugteren, S. & Samsom, J. N. Secretory Leukocyte Protease Inhibitor (SLPI) in mucosal tissues: protects against inflammation, but promotes cancer. *Cytokine Growth Factor Rev.* **59**, 22–35 (2021).
18. Moreau, T. et al. Multifaceted roles of human elafin and secretory leukocyte proteinase inhibitor (SLPI), two serine protease inhibitors of the chelonian family. *Biochimie* **90**, 284–295 (2008).
19. Sallenave, J. M. The role of secretory leukocyte proteinase inhibitor and elafin (elastase-specific inhibitor/skin-derived antileukoprotease) as alarm antiproteases in inflammatory lung disease. *Respir. Res.* **1**, 87–92 (2000).
20. Marino, R. et al. Secretory leukocyte protease inhibitor plays an important role in the regulation of allergic asthma in mice. *J. Immunol.* **186**, 4433–4442 (2011).
21. Afacan, B. et al. Salivary secretory leukocyte protease inhibitor levels in patients with stage 3 grade C periodontitis: a comparative cross-sectional study. *Sci. Rep.* **12**, 21267 (2022).



22. Kretschmar, S. et al. Protease inhibitor levels in periodontal health and disease. *J. Periodontol. Res.* **47**, 228–235 (2012).
23. Hiyoshi, T. et al. Neutrophil elastase aggravates periodontitis by disrupting gingival epithelial barrier via cleaving cell adhesion molecules. *Sci. Rep.* **12**, 8159 (2022).
24. Okazaki, M., Yamada, Y., Nishimoto, N., Yoshizaki, K. & Mihara, M. Characterization of anti-mouse interleukin-6 receptor antibody. *Immunol. Lett.* **84**, 231–240 (2002).
25. Uehara, T. et al. Delivery of RANKL-binding peptide OP3-4 promotes BMP-2-induced maxillary bone regeneration. *J. Dent. Res.* **95**, 665–672 (2016).
26. Salazar, V. S., Gamer, L. W. & Rosen, V. BMP signalling in skeletal development, disease and repair. *Nat. Rev. Endocrinol.* **12**, 203–221 (2016).
27. Arima, H. et al. Blockade of IL-6 signaling by MR16-1 inhibits reduction of docosahexaenoic acid-containing phosphatidylcholine levels in a mouse model of spinal cord injury. *Neuroscience* **269**, 1–10 (2014).
28. Miyazaki, T., Miyauchi, S., Anada, T., Imaizumi, H. & Suzuki, O. Evaluation of osteoclastic resorption activity using calcium phosphate coating combined with labeled polyanion. *Anal. Biochem.* **410**, 7–12 (2011).
29. Quarles, L. D., Yohay, D. A., Lever, L. W., Caton, R. & Wenstrup, R. J. Distinct proliferative and differentiated stages of murine MC3T3-E1 cells in culture: an in vitro model of osteoblast development. *J. Bone Min. Res.* **7**, 683–692 (1992).
30. Addison, W. N. et al. Extracellular matrix mineralization in murine MC3T3-E1 osteoblast cultures: an ultrastructural, compositional and comparative analysis with mouse bone. *Bone* **71**, 244–256 (2015).
31. Yuh, D. Y. et al. The secreted protein DEL-1 activates a beta3 integrin-FAK-ERK1/2-RUNX2 pathway and promotes osteogenic differentiation and bone regeneration. *J. Biol. Chem.* **295**, 7261–7273 (2020).
32. Morimoto, A. et al. SLPI is a critical mediator that controls PTH-induced bone formation. *Nat. Commun.* **12**, 2136 (2021).
33. Fujita, R. et al. Anti-interleukin-6 receptor antibody (MR16-1) promotes muscle regeneration via modulation of gene expressions in infiltrated macrophages. *Biochim. Biophys. Acta* **1840**, 3170–3180 (2014).
34. Kantarci, A., Hasturk, H. & Van Dyke, T. E. Host-mediated resolution of inflammation in periodontal diseases. *Periodontol. 2000* **40**, 144–163 (2006).
35. Nunez, J., Vignoletti, F., Caffesse, R. G. & Sanz, M. Cellular therapy in periodontal regeneration. *Periodontol. 2000* **79**, 107–116 (2019).
36. Nanci, A. & Bosshardt, D. D. Structure of periodontal tissues in health and disease. *Periodontol. 2000* **40**, 11–28 (2006).
37. Schwartz, Z., Goultschin, J., Dean, D. D. & Boyan, B. D. Mechanisms of alveolar bone destruction in periodontitis. *Periodontol. 2000* **14**, 158–172 (1997).
38. Taggart, C. C. et al. Secretory leucoprotease inhibitor binds to NF-kappaB binding sites in monocytes and inhibits p65 binding. *J. Exp. Med.* **202**, 1659–1668 (2005).
39. Asagiri, M. & Takayanagi, H. The molecular understanding of osteoclast differentiation. *Bone* **40**, 251–264 (2007).
40. Choi, B. D. et al. Secretory leukocyte protease inhibitor promotes differentiation and mineralization of MC3T3-E1 preosteoblasts on a titanium surface. *Mol. Med. Rep.* **14**, 1241–1246 (2016).
41. Lin, C. C. & Chang, J. Y. Pathway of oxidative folding of secretory leukocyte protease inhibitor: an 8-disulfide protein exhibits a unique mechanism of folding. *Biochemistry* **45**, 6231–6240 (2006).
42. Tamura, H., Maekawa, T., Hiyoshi, T. & Terao, Y. Analysis of experimental ligature-induced periodontitis model in mice. *Methods Mol. Biol.* **2210**, 237–250 (2021).
43. Tamura, H. et al. Effects of erythromycin on osteoclasts and bone resorption via DEL-1 induction in mice. *Antibiotics* **10**, 312 (2021).

## Acknowledgements

We express our sincere gratitude to Chugai Pharmaceutical and Prof. T.K. for supplying the anti-mouse IL-6 receptor antibody. We thank Dr F.T., Dr R.S., and Dr Y.Y. for advice regarding our experiments. This work was supported by grants from the Japan Society for the Promotion of Science KAKENHI (grant numbers 20H03858, 22K19614, 22K09923, 20K09903, 22H03267, 22KJ1445, and 23H00445). This work was supported by JST and Niigata University (Fellowship Program No. JPMJFS2114-156695-J23H0004). These funders had no role in the study design, data collection, and interpretation, or the decision to submit the manuscript for publication.

## Author contributions

K.S. and Y.T. conceptualization; K.S., H.D., S.H., and T.I. formal analysis; K.S. and T.I. investigation; K.S. and H.D. writing—original draft; H.D., T.M., and Y.T. writing—review & editing; M.T., K.T., and Y.T. supervision; Y.T. project administration; K.S., H.D., S.H., T.M., T.I., and Y.T. funding acquisition.

## Competing interests

The authors declare no competing interest.

## Additional information

**Supplementary information** The online version contains supplementary material available at <https://doi.org/10.1038/s42003-025-08197-3>.

**Correspondence** and requests for materials should be addressed to Yutaka Terao.

**Peer review information** *Communications Biology* thanks J.B. and I.K. for their contribution to the peer review of this work. Primary handling editor: O.B. A peer review file is available.

**Reprints and permissions information** is available at <http://www.nature.com/reprints>

**Publisher's note** Springer Nature remains neutral with regard to jurisdictional claims in published maps and institutional affiliations.

**Open Access** This article is licensed under a Creative Commons Attribution-NonCommercial-NoDerivatives 4.0 International License, which permits any non-commercial use, sharing, distribution and reproduction in any medium or format, as long as you give appropriate credit to the original author(s) and the source, provide a link to the Creative Commons licence, and indicate if you modified the licensed material. You do not have permission under this licence to share adapted material derived from this article or parts of it. The images or other third party material in this article are included in the article's Creative Commons licence, unless indicated otherwise in a credit line to the material. If material is not included in the article's Creative Commons licence and your intended use is not permitted by statutory regulation or exceeds the permitted use, you will need to obtain permission directly from the copyright holder. To view a copy of this licence, visit <http://creativecommons.org/licenses/by-nc-nd/4.0/>.

© The Author(s) 2025